

Nuclear Tracks Morphology Study Using Raman Methodology

MARIANA CERDA Z.¹, J. A. AZAMAR-BARRIOS¹, C. VÁZQUEZ LÓPEZ^{2*},
R. FRAGOSO-SORIANO², B. E. ZENDEJAS-LEAL², J. RURIK FARÍAS³,
J. I. GOLZARRI⁴, G. ESPINOSA⁴

¹Departamento de Física Aplicada, Centro de Investigación y de Estudios Avanzados del IPN, Unidad Mérida.

²Departamento de Física. Centro de Investigación y de Estudios Avanzados del IPN, Ciudad de México

³Instituto de Ingeniería y Tecnología Universidad Autónoma de Cd. Juárez, Chih.

⁴Instituto de Física. Universidad Nacional Autónoma de México. Circuito de la Investigación Científica, Ciudad Universitaria. 04520, Ciudad de México

*Email: cvlopez@fis.cinvestav.mx

Published online: August 08, 2016,

The Author(s) 2016. This article is published with open access at www.chitkara.edu.in/publications

Abstract In this work, a new methodology for rendering profiles of etched nuclear tracks is presented, using confocal micro-Raman spectrometry instrumentation. The precise profile of etched nuclear tracks with normal and/or angular incidence of the particle can be determined in few minutes, with a great visual and numerical resolution, that means a quantitative and qualitative simultaneous chemical and morphology characterization with the Raman technique. The Raman image routine is designed to acquire at each image pixel a complete Raman spectrum. This is a mapping of the functional groups that form the polymeric structure, which may be broken by the damage caused by the incident radiation and/or the etching process.

Keywords: Micro-Raman spectroscopy, CR-39 SSNTD, Track morphology.

1. INTRODUCTION

The morphology of etched nuclear tracks in solids is very important, since it reveals the interaction of incident ions with matter. The rate of kinetic energy loss is of particular interest. Track profiles in plastic detectors have been studied by means of confocal microscopy[10], holographic digital microscopy [8], and by cutting the sample nearly parallel to the track axis,

Journal of Nuclear
Physics, Material
Sciences, Radiation and
Applications
Vol-4, No-1,
August 2016
pp. 241–250

Mariana Cerda, Z.
Azamar-Barrios, A.
Vázquez López, C.
Fragoso-Soriano, R.
Zendejas-Leal, B.E.
Rurik Farías, J.
Golzari, J.I.
Espinosa, G.

and then using optical microscopy [6]. Atomic force microscopy (AFM) has also been used by many authors [3, 7, 11, 13]. In fact, AFM is considered the best method to obtain etched track profiles. However, there is a serious limitation in the AFM instrumentation that is necessary to remark: the particle incidence should be perpendicular to the polymeric detector. Otherwise, when the particle incidence is not normal, the AFM tip does not properly scan the track profile, as shown in Figure 1 [5]. The red line is the AFM profile obtained, because during the scan process the sample and the tip are in contact in different places at the same time. In addition, the track cavity bottom is out of reach the AFM tip.

In the last years, IR[12], FT-IR[1], UV-Vis [4] and Raman [9] spectroscopic techniques have been used to study nuclear tracks detectors. These techniques provide a lot of information about chemical structure being able to observe changes in the molecular structure and/or polymeric morphology after the materials are irradiated by ionizing particles.

In this work, it is demonstrated the ability of confocal Raman instrumentation to obtain 2-D and 3-D images of etched nuclear tracks in CR-39, with normal and/or angular particle incidence. Thus, it provides fundamental information such as the track diameter, depth of damage and the profile of the mapped region.

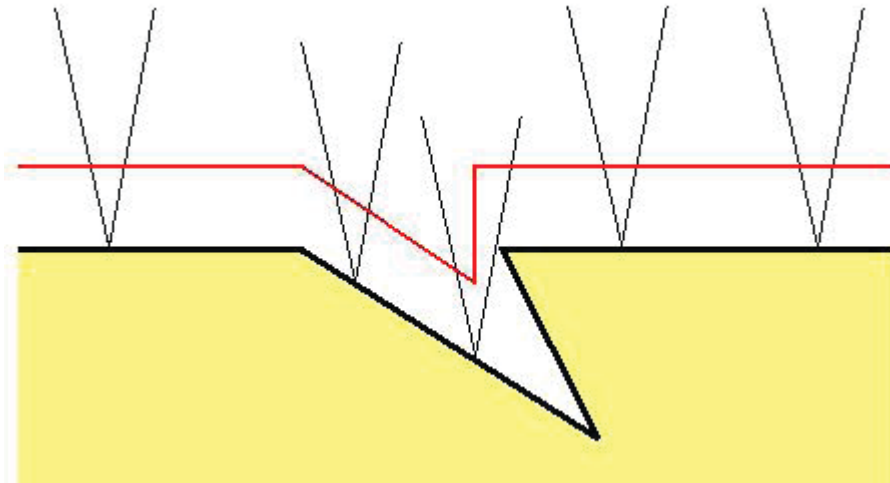


Figure 1: AFM does not raster scan properly the profile of tracks from non-normal incident particles.

2. INSTRUMENTATION

CR-39 Lantrack (9 mm x 19 mm chips) and 500 μm thickness was used as detecting material. An emitter source of alpha particles of 5.15 MeV was selected as track generator radioactive source. The exposure was made in air. The detectors were chemically etched under the same conditions following the very well established procedure [2], in 6.25 M KOH solution at $60\pm 1^\circ\text{C}$, at different etching times. The full set of detectors was washed and dried with the same process and conditions. After these procedures, the detectors were analyzed with the micro-Raman instrument.

In Figure 2, a schematic setup of the system is shown. Two kinds of equipment were used: Instrument 1: WITecAlpha300 RA (CINVESTAV-IPN) with a 632.8 nm laser, and the software Witec Project FOUR, and Instrument 2: Thermo Scientific DXR (IF-UNAM) with a 532 nm laser, and the spectra were analyzed with the OMNIC 8.1 Thermo Fisher Scientific Inc. software.

In these systems, the laser light is delivered via single mode optical fiber. This type of fiber transmits only a single transversal mode (Gaussian beam), which can be focused to a diffraction limited spot. The light reflected by the sample is collected by the same objective and is directed as a parallel beam

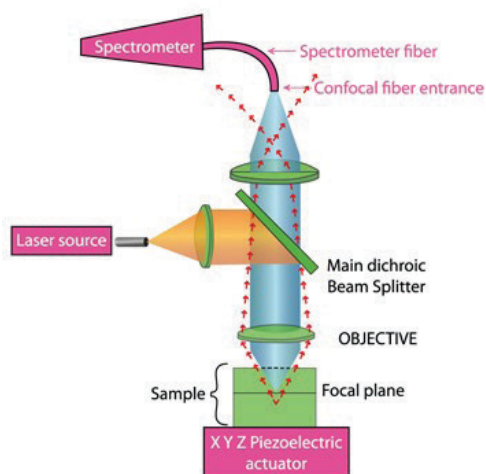


Figure 2: A scheme of the confocal Raman system. No significant detection occurs from out-of-focus illuminated regions that may emit photons indicated by red arrows.

Mariana Cerda, Z.
Azamar-Barrios, A.
Vázquez López, C.
Fragoso-Soriano, R.
Zendejas-Leal, B.E.
Rurik Farías, J.
Golzarri, J.I.
Espinosa, G.

toward the top of the microscope. Here, the light is focused onto a multi-mode optical fiber. The core of this multi-mode optical fiber acts as a pinhole for confocal microscopy. The laser is raster-scanned across the sample by scanning the sample in all axes and the image is acquired line by line. The confocal fiber acts as a spatial filter, blocking the fluorescence and/or Raman photons originated outside of the focal spot of the objective lens, as indicated by the red arrows in Figure 2.

Two cases are considered in this work: tracks from perpendicularly incident particles in which the detector was exposed to the alpha source at 2.11 cm distance that corresponds to an alpha incident energy W of 3 MeV (TRIM code calculation [14]) and an etching time of 4 h; and tracks from obliquely incident particles at an angle of 45° .

The images are calculated by isolating spectral characteristics (height, width, peak position, etc.) of the obtained Raman spectra. The respective image processor software converts the Raman intensity of the pixel in a color scale.

In this work, the spectral characteristic chosen to be isolated is the strongest band at 2960 cm^{-1} , corresponding to the CR-39 polymeric functional group CH_2 with symmetric stretching mode (Figure 3).

3. EXPERIMENTAL RESULTS AND DISCUSSION

By using Instrument 1, the optical image of the etched tracks shown in Figure 4 was obtained. In order to calculate the depth-profiling a red line across the central track is programmed to be analyzed by the instrument.

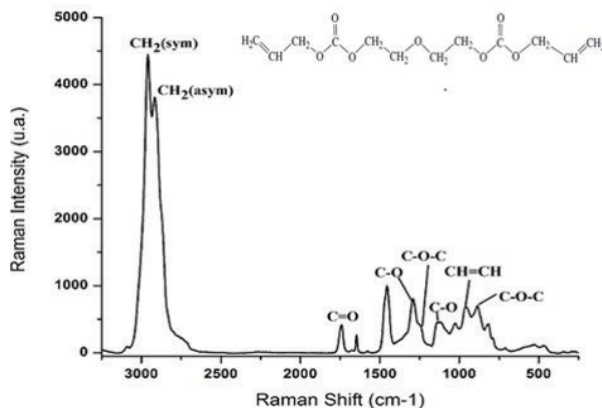


Figure 3: Raman spectrum corresponding to CR-39 detectors and CR-39 polymeric structure.

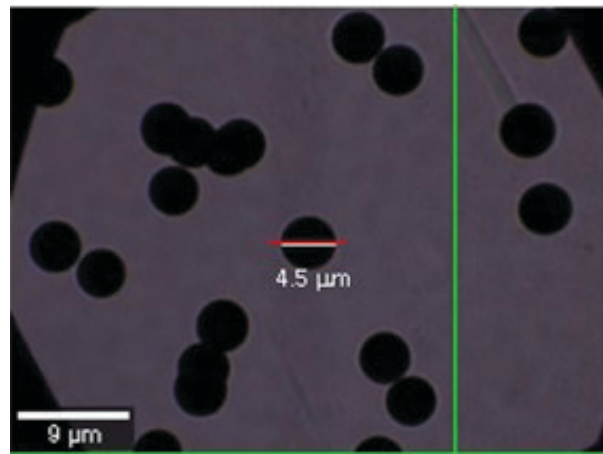


Figure 4: Optical image of etched nuclear tracks corresponding to alpha particles with normal incidence.

The instrument is then programmed to obtain complete Raman spectra across the red line at different depths. The resulting image is shown in Figure 5. The black color corresponds to the absence of CR-39 material, i.e. the conical cavity of the etched track is clearly obtained. Another feature worth to be observed are the Raman spectral lines at different positions of the profile: There is no appreciable change in the relative peaks size at all. The change occurs only in the whole spectra intensity.

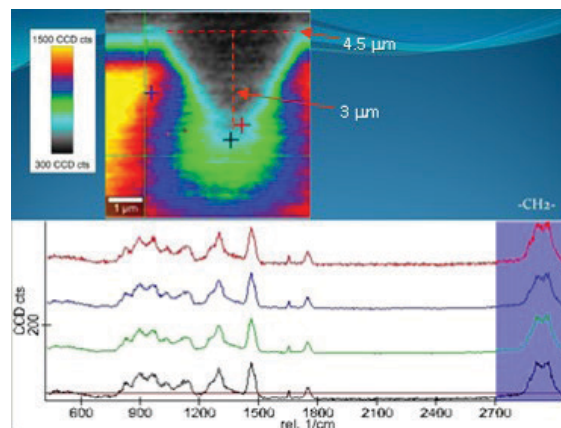


Figure 5: Micro-Raman image (Above) obtained by isolating the CH_2 stretching modes, indicated by the blue shadow of the spectra shown below. These spectra were obtained at the points in the image indicated by symbol +.

Mariana Cerda, Z.
Azamar-Barrios, A.
Vázquez López, C.
Fragoso-Soriano, R.
Zendejas-Leal, B.E.
Rurik Farías, J.
Golzari, J.I.
Espinosa, G.

In Figure 5 the measurement of diameter ($4.5\ \mu\text{m}$) and the track depth ($3\ \mu\text{m}$) is indicated. The diameter corresponds to that obtained in Figure 4.

By using Instrument 2, the results shown in Figure 6 were obtained, corresponding to normal incidence of alpha particles. In Figure 6a) an optical image of the sample is shown. The track to be analyzed is marked with a red square. In Figure 6b) a 2-D mapping of the chosen track is shown. The color scale corresponds to the intensity of the Raman spectra, which decreases with depth towards the center of the track. In Figure 6c) the 3-D representation from the 2-D mapping is shown. In this figure the Z axis corresponds to the Raman intensity.

In Figure 6b) the measurement of the diameter of the nuclear track is indicated, resulting $5.3\ \mu\text{m}$ that may be directly compared with that obtained with the optical microscope.

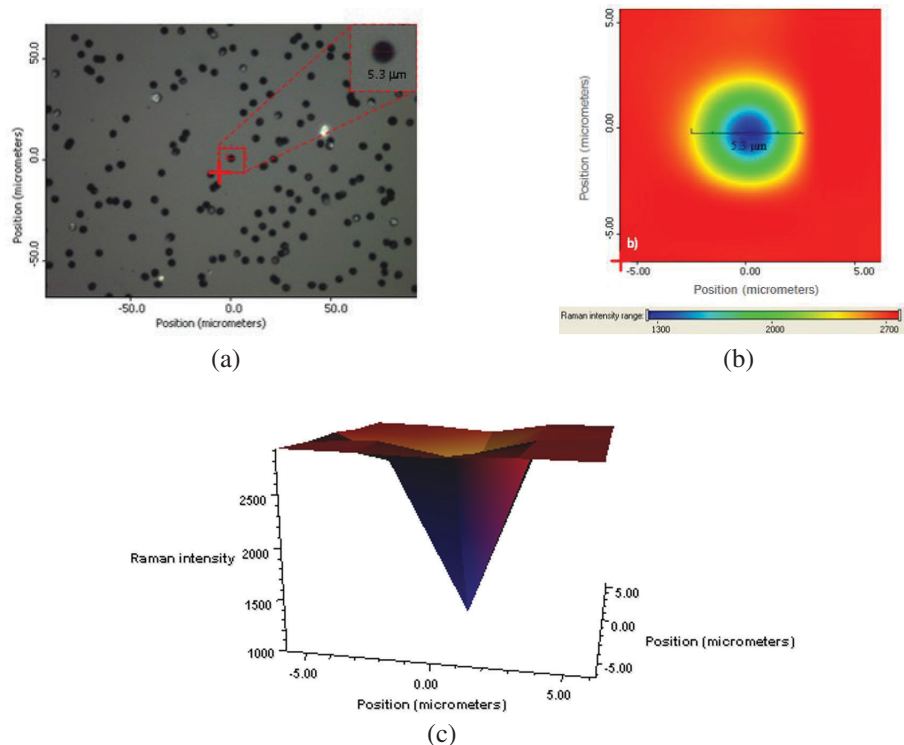


Figure 6: Micro-Raman images of a track from a normal incident alpha particle. **Figure 6a):** Optical microscope image. **Figure 6b):** 2-D mapping of the previous marked track with color scale indicating Raman intensity. **Figure 6c):** 3D representation of Figure 6b).

The case where the alpha particle is not perpendicularly incident is shown in Figure 7, using the Instrument 2. In this case the incidence energy $W=2.5$ MeV and the etching time 4 h. The optical image is shown in Figure 7a). In Figure 7b) a 2-D mapping of the track is shown. The color scale corresponds to the intensity of the Raman spectra, as in Figure 6. In this case, the signal decreases with depth towards the right edge of the track. In Figure 7c) the 3-D representation from the 2-D mapping is shown. In this figure the Z axis corresponds to the Raman spectrum intensity, as before, where the oblique trajectory is clearly shown.

Similar measurements were performed using Instrument 1. The results are shown in Figure 8. The optical image 8a) shows an elliptical track. The Raman depth profiling was obtained across the red line, and the result is shown in Figure 8b). In Figure 8c) a 2-D image of the track is shown, in which regularly spaced isoclines of the Raman intensity are calculated. A 3-D representation of the Raman intensity of this image is presented in Figure 8d). It is interesting to note that this figure provides a 3-D topographical map of the etched nuclear track.

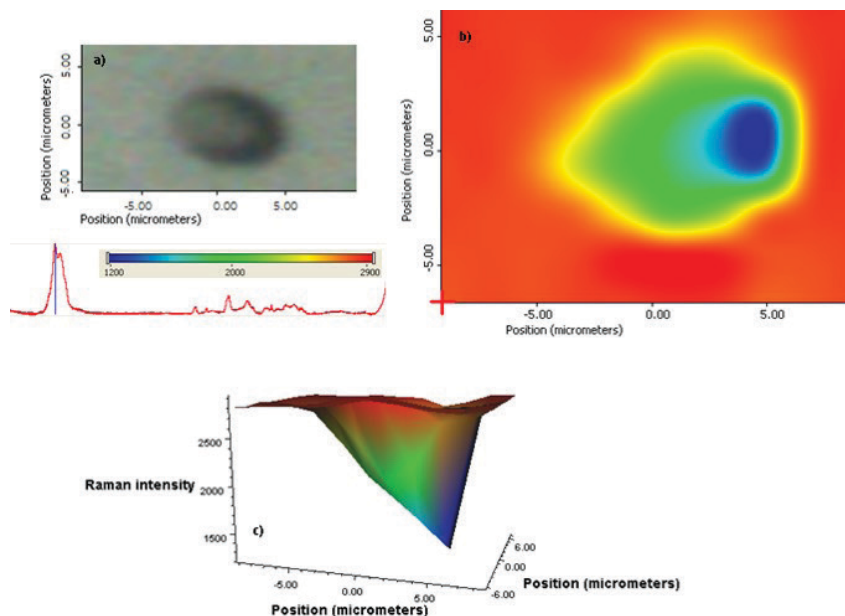


Figure 7: Micro-Raman images of a track from a non perpendicular incident alpha particle. **Figure 7a):**Optical image zoom of the nuclear track. **Figure 7b):**Raman 2-D mapping of the track shown in Figure 7a). The color scale indicates Raman intensity. **Figure 7c):** 3D representation of image shown in Figure 7b).

Mariana Cerda, Z.
Azamar-Barrios, A.
Vázquez López, C.
Fragoso-Soriano, R.
Zendejas-Leal, B.E.
Rurik Farías, J.
Golzarri, J.I.
Espinosa, G.

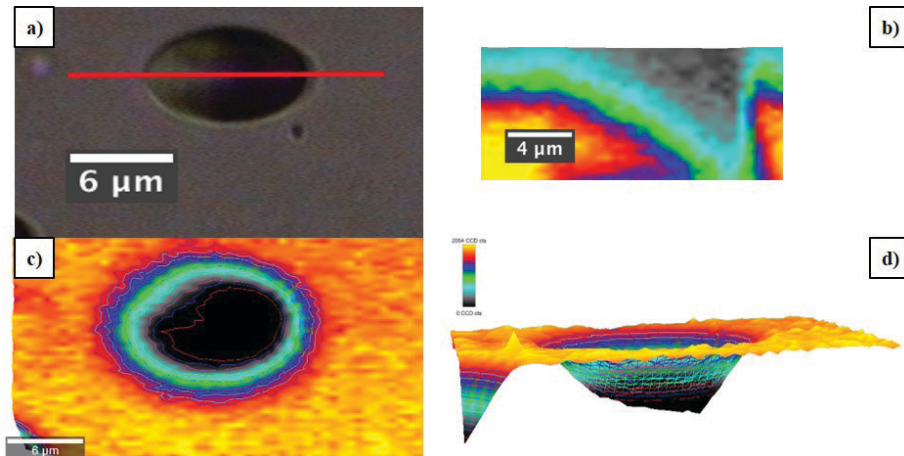


Figure 8: Micro-Raman images of a track from an oblique incident alpha particle, obtained in a WITec Alpha 300. **Figure 8a)**: Optical image of the selected nuclear track. **Figure 8b)**: The Raman depth profiling across the red line in Figure 8a). **Figure 8c)**: 2-D Raman image from top view, and **Figure 8d)**: 3-D Raman intensity mapping of image 8c), which corresponds to a topographical image with the same bar scale as that in Figure 8c).

4. CONCLUSIONS

To the best of our knowledge, this is the first work that Micro-Raman images of etched nuclear tracks in CR-39 detectors were obtained. This technique allows us to perform a complete reconstruction of the etched track morphology, enabling further characterizations. With this, the study of different particles or reactions, like (n- α) or (n-p), can be performed with the morphologic information of a specific track, such as the diameter, trajectory and range in the material.

Micro-Raman confocal spectroscopy is a useful tool to study nuclear tracks morphology from particles at normal as well as non-normal incidence.

ACKNOWLEDGEMENTS

The authors would like to thank Cristina Zorrilla Cangas (*Laboratorio de Materiales Avanzados, IF-UNAM*) for technical help in Raman spectroscopy, and to A. García, M. Veytia, P. Carrasco, N. Gonzalez, J. Martínez, and M. Cuautle, for their technical help. This work was partially supported by *Dirección General del Personal Académico de la UNAM*, Project IN103316.

REFERENCES

- [1] Chong, C., Ishak, I., Mahat, R. & Amin, Y. UV-VIS and FTIR spectral studies of CR-39 plastics irradiated with X-rays. *Radiation Measurements*, **28(1-6)**, 119-122 (1997). [http://dx.doi.org/10.1016/S1350-4487\(97\)00051-6](http://dx.doi.org/10.1016/S1350-4487(97)00051-6)
- [2] Espinosa, G., Gammage, R., Golzarri, J. & Casta-o, V. Studies on the interaction of alpha particles with polycarbonate materials. *Int. J. Polym. Mater.*, Issue **40**, 87-95 (1998).
- [3] Espinosa, G., Jacobson, I., Golzarri, J.I., Vázquez, C., Fragoso, R. & Santos, E. Analysis of the formed track in solid state materials using atomic force microscopy. *Radiation Protection Dosimetry*, **101(1-4)**, 89-92 (2002). <http://dx.doi.org/10.1093/oxfordjournals.rpd.a006066>
- [4] Fawzy Eissa, M., et al. Optical Properties of CR-39 Track Etch Detectors Irradiated by Alpha Particles with Different Energies. *Journal of Materials Science and Engineering*, **5**, 26-31 (2011).
- [5] Félix-Bautista, R., Hernández-Hernández, C., Zendejas-Leal, B.E., Fragoso, R., Golzarri, J.I., Vázquez-López, C. & Espinosa, G. Evolution of etched nuclear track profiles of alpha particles in CR-39 by atomic force microscopy. *Radiation Measurements*, **50**, 197-200 (2013). <http://dx.doi.org/10.1016/j.radmeas.2013.01.002>
- [6] Mosier-Boss, P. et al. Comparison of SEM and optical analyses of DT neutron tracks in CR-39 detectors. *Radiation Measurements*, Issue **47**, 57-66 (2012). <http://dx.doi.org/10.1016/j.radmeas.2011.10.004>
- [7] Nikezic, D. et al. Feasibility and limitation of track studies using atomic force microscopy. *Nuclear Instruments and Methods in Physics Research*, **197-B**, 293-300 (2002). [http://dx.doi.org/10.1016/S0168-583X\(02\)01480-5](http://dx.doi.org/10.1016/S0168-583X(02)01480-5)
- [8] Palacios, F. et al. 3D image reconstruction of transparent microscopic objects using digital holography. *Optics Communications*, Issue **248**, 41-50 (2005). <http://dx.doi.org/10.1016/j.optcom.2004.11.095>
- [9] Stuaní Pereira, L. A. et al. Micro-Raman Spectroscopic Characterization of a CR-39 Detector. *Applied Spectroscopy*, **67(4)**, 404-408 (2013). <http://dx.doi.org/10.1366/12-06741>
- [10] Vaginay, F. et al. 3-D confocal microscopy track analysis: a promising tool for determining CR-39 response function. *Radiation Measurements*, Volume **34**, 123 (2001). [http://dx.doi.org/10.1016/S1350-4487\(01\)00136-6](http://dx.doi.org/10.1016/S1350-4487(01)00136-6)
- [11] Yamamoto, M. et al. Atomic force microscopic analysis of heavy ion tracks in CR-39. *Nuclear Instruments and Methods in Physics Research*, **152-B**, 349-356 (1999). [http://dx.doi.org/10.1016/S0168-583X\(99\)00121-4](http://dx.doi.org/10.1016/S0168-583X(99)00121-4)
- [12] Yamauchi, T., Takada, S., Ichijo, H. & Oda, K. Raman and near-IR study on proton irradiated CR-39 detector and the effect of air-leak on damage formation. *Radiation Measurements*, Issue **34**, 69-73 (2001). [http://dx.doi.org/10.1016/S1350-4487\(01\)00123-8](http://dx.doi.org/10.1016/S1350-4487(01)00123-8)

-
- Mariana Cerda, Z. [13] Yasuda, N. et al. Measurement of bulk etch rate of CR-39 with atomic force
Azamar-Barrios, A. microscopy. Nuclear Instruments and Methods in Physics Research, **142-B**,
Vázquez López, C. 111-116 (1998). [http://dx.doi.org/10.1016/S0168-583X\(98\)00267-5](http://dx.doi.org/10.1016/S0168-583X(98)00267-5)
Fragoso-Soriano, R. [14] Ziegler J., Biersack, J. & Littmark U. The Stopping and Range of Ions in Solids,
Zendejas-Leal, B.E. Pergamon Press, Oxford (1985).
Rurik Farías, J.
Golzarri, J.I.
Espinosa, G.
-